


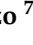


Article

Can New Ultrasound Imaging Techniques Improve Breast Lesion Characterization? Prospective Comparison between Ultrasound BI-RADS and Semi-Automatic Software “SmartBreast”, Strain Elastography, and Shear Wave Elastography

Olga Guiban ^{1,2,*}, Antonello Rubini ², Gianfranco Vallone ³, Corrado Caiazzo ⁴, Marco Di Serafino ⁵ , Federica Pediconi ¹ , Laura Ballesio ¹, Federica Trenta ¹, Corrado De Vito ⁶, Arenta Shkelqimi ¹, Ludovica Costanzo ⁷, Daniele Fresilli ¹ , Veronica Rizzo ¹ , Vito Cantisani ^{1,*} and Massimo Vergine ⁷

¹ Department of Radiological Sciences, Oncology and Pathology, Policlinico Umberto I, Sapienza University of Rome, 00100 Rome, Italy

² Division of Radiology and Diagnostic Imaging, ASL Rome, 00184 Rome, Italy

³ Department of Life and Health, University of Molise “V. Tiberio”, 86100 Campobasso, Italy

⁴ Radiology Unit, PSP Corso Vittorio Emanuele ASL Napoli 1, 80122 Naples, Italy

⁵ Department of General and Emergency Radiology, “Antonio Cardarelli” Hospital, 80131 Naples, Italy

⁶ Department of Public Health and Infectious Diseases, Sapienza University, 00189 Rome, Italy

⁷ Department of Surgical Sciences, Sapienza University, 00189 Rome, Italy;

massimo.vergine@uniroma1.it (M.V.)

* Correspondence: olga.guiban@uniroma1.it (O.G.); vito.cantisani@uniroma1.it (V.C.)



Citation: Guiban, O.; Rubini, A.; Vallone, G.; Caiazzo, C.; Di Serafino, M.; Pediconi, F.; Ballesio, L.; Trenta, F.; De Vito, C.; Shkelqimi, A.; et al. Can New Ultrasound Imaging Techniques Improve Breast Lesion Characterization? Prospective Comparison between Ultrasound BI-RADS and Semi-Automatic Software “SmartBreast”, Strain Elastography, and Shear Wave Elastography. *Appl. Sci.* **2023**, *13*, 6764. <https://doi.org/10.3390/app13116764>

Academic Editor: Theodore E. Matikas

Received: 25 March 2023

Revised: 30 May 2023

Accepted: 31 May 2023

Published: 2 June 2023



Copyright: © 2023 by the authors. Licensee MDPI, Basel, Switzerland. This article is an open access article distributed under the terms and conditions of the Creative Commons Attribution (CC BY) license (<https://creativecommons.org/licenses/by/4.0/>).

Abstract: Background: Ultrasound plays a crucial role in early diagnosis of breast cancer. The aim of this research is to evaluate the diagnostic performance of BI-RADS classification in comparison with new semi-automatic software Resona R9, Mindray, “SmartBreast” and strain elastography (SE), point shear wave (pSWE), and 2D shear wave (2D SWE) Elastography for breast lesion differentiation. Methods: Ninety-two breast nodules classified according to BI-RADS lexicon by an expert radiologist were evaluated by a second investigator with B-mode ultrasound, color Doppler, “SmartBreast”, and elastography. Histopathology was considered the gold standard. Results: The agreement between software and investigator was excellent in the identification of the posterior features of breast masses (Cohen’s $k = 0.94$), good for shape and vascular signal (Cohen’s k , respectively, of 0.6 and 0.65), poor for orientation, margins, and echo pattern (Cohen’s k , respectively, of 0.28, 0.33 and 0.48), moderate for dimensions (Lin’s correlation coefficient of 0.90, $p = 0.07$). SE showed a greater area under curve (AUC) than pSWE and 2D SWE (0.84, 0.64, and 0.61, respectively), with a greater specificity and a comparable sensitivity to pSWE (respectively, of 0.86 and 0.55, 0.81 and 0.84). Conclusions: SE improved the diagnostic performance of BI-RADS classification more than pSWE and 2D SWE; “SmartBreast” showed good agreement only for shape and vascularization but not for the other ultrasound features of breast lesions.

Keywords: ultrasound; computer-aided diagnosis; “SmartBreast”; strain elastography; shear wave elastography; pSWE; 2D SWE

1. Introduction

Breast cancer is the most common cancer among women [1], and it is a leading health concern among women due to its high mortality and morbidity rates [2]. Different imaging techniques for breast lesion characterization, alone or in combination, have been extensively evaluated with generally high sensitivity despite limited specificity values in the distinction between benign and malignant masses. Breast cancer is a heterogenous disease with various histologic subtypes, molecular profiles, behaviors, and responses to therapy. Among benign tumors, the most frequent lesions are fibroadenomas, while infiltrating

ductal carcinoma is the most common malignant lesion. After the histologic assessment and diagnosis of an invasive breast carcinoma, the use of biomarkers, multigene expression assays, and mutation profiling may be used in order to choose the proper treatment. Currently, mammography is widely recognized as the best technique in the early detection of breast cancer [3]. It allows a complete and repeatable breast evaluation with quality control and has maximal sensitivity values, especially in the initial phase of breast tumors. These features make mammography the best screening method in patients over 40 years of age. However, mammography has limitations. In a recent review, Humphrey et al. [4] estimated the sensitivity for mammography for a one-year screening interval to be between 71% and 96%, with lower sensitivity observed in younger compared with older women. Factors known to affect mammographic sensitivity include breast density (being clearly better in fatty breasts), use of hormone replacement therapy, poor image quality, number of views, and the experience and skill of the interpreting physician. Greater experience in interpreting mammograms, independent double reading, and computer-aided detection have all been shown to improve mammographic sensitivity. Mammographic specificity was estimated between 94% and 97%. Most women with a false positive result on screening mammography usually undergo additional mammograms, ultrasound studies, or physical examinations, and the majority of these women are subsequently determined not to have breast cancer. This fact leads to an increase in healthcare costs and has a negative impact on patients' anxiety. Another problem of periodic mammography screening is overtreatment of benign lesions or the detection of less aggressive ductal carcinoma in situ (DCIS) in elderly patients who do not benefit from a reduction of mortality risk but may have a reduction of life quality from the treatment. Finally, another disadvantage of mammography is that it cannot be used as a periodic screening in young patients (under 35 years) and, in particular, in young patients with genetic mutations, such as BRCA-1 and BRCA-2 mutations, and in patients who underwent previous chest radiation therapy at a young age. All of these categories, which have a high risk for breast cancer but at the same time have increased radiosensitivity, should be screened only with ultrasound and magnetic resonance imaging, because neither uses ionizing radiation [5].

Ultrasound (US) was proven to be very useful in breast lesion differentiation, being a non-invasive, reproducible, and cost-effective technique, and became the first-line imaging in young women (especially before the age of 40) and the complementary method to mammography in older women with dense breast structure [6]. Ultrasound is also a useful tool in carrying out biopsy procedures. Its main limitations consist of being an operator-dependent technique and the substantial overlap of morphologic ultrasound features between benign and malignant lesions.

With the introduction of the Breast Imaging Reporting and Data System (BI-RADS) for US [7], the criteria for describing and classifying breast nodules were standardized with good diagnostic performance.

Newly established US and elastography techniques have been studied as an additional method to analyze tissue stiffness in order to improve US examination specificity in the characterization of focal breast masses [8–10]. The European Federation of Ultrasound in Medicine and Biology (EFSUMB) and the World Federation of Ultrasound in Medicine and Biology (WFUMB) described US elastography and published their guidelines about physical principles, clinical indications, and limitations in several fields, including breast imaging [10]. Strain elastography (SE) and shear wave elastography (SWE) are the two main methods used in breast imaging.

SE is a qualitative and semi-quantitative technique based on compression applied by an external source (mechanical compression performed by the transducer) with the transducer kept still and perpendicular to the body surface. In SE, the absolute value cannot be calculated since the force degree applied during the compression is not known, and the deformation of the lesion can be represented as a relationship with a reference tissue (fat tissue in the breast) and visualized by a color or a gray scale. The stiffness scale has color values ranging from red (soft tissue) to blue (stiff areas), passing through green

(intermediate stiffness). For a semi-quantitative as well as for a qualitative evaluation (color map), the strain ratio (SR) may be calculated considering the deformability ratio between the tumor and the breast fat [9,10].

SWE is a different quantitative method in which the force of acoustic radiation generates shear waves in the tissue. This kind of elastography provides quantitative information (measured in kPa or m/s) shown also as a color map of the lesion and of the neighboring tissues in real time. SWE can be further divided into 2D-SWE (sound touch elastography (STE)) and point shear-wave elastography (pSWE, sound touch quantification (STQ)), in which tissue stiffness is respectively represented as the mean elasticity of the region of interest (ROI) or as a measurement of each pixel included in the field of view.

Multiple studies evaluating the possible role of SWE and SE have reported that breast elastography is useful for differentiating benign from malignant lesions and could potentially reduce unnecessary biopsies by improving the accuracy of breast US [10–12]. However, no specific recommendations have been provided by guidelines regarding the superiority of one method over the other [13].

Recent studies have evaluated the potential role of computer-aided diagnosis (CAD) and artificial intelligence systems in supporting breast imaging in mammography, ultrasound, and MRI, respectively, emphasizing the variability of the results of different papers and the need for large-scale cohort studies [14].

“SmartBreast” is a new semi-automatic software able to carry out a multiplanar analysis of breast lesions and provide an intelligent classification and reporting tool, according to the BI-RADS lexicon.

The purpose of our study was to compare the diagnostic performance of these new ultrasound techniques in the differentiation of benign and malignant breast lesions, in accordance with the BI-RADS classification, evaluating the agreement between “SmartBreast” and the radiologist, and the diagnostic accuracy of elastography performed with strain ratio (SE, SR), pSWE, and 2D SWE.

2. Materials and Methods

The whole study was carried out in accordance with the Declaration of Helsinki. Informed patients’ consent was obtained for this prospective study. Permission for patients’ medical records review was obtained from the hospital. Between November 2021 and September 2022, 85 patients aged between 12 and 85 years (mean age 52 ± 12 SD) were enrolled, for a total of 92 focal breast lesions that were evaluated by a radiologist with extensive experience in breast imaging (at least 10 years) who provided the BI-RADS category for each lesion, in accordance with the latest ACR BI-RADS 2013 edition lexicon. All patients underwent a biopsy.

The inclusion criteria of the study were: all ultrasound-detectable breast masses were candidates for biopsy and classified with a BI-RADS score between 3 and 5 (probably benign nodules but of first finding and/or growth at follow-up, nodules of uncertain category, or lesions with suspected malignancy).

The exclusion criteria were: benign breast nodules that did not undergo biopsy or follow-up, patient’s refusal to perform core-needle biopsy, biopsy performed before ultrasound examination in less than 1 month, clearly benign nodules (BI-RADS 2), or mixed lesions with the solid component poorly assessable due to the elastographic artifacts linked to the prevalent cystic component.

All breast nodules included in the study were subsequently evaluated by a second investigator by means of a B-mode ultrasound, color Doppler, and analysis performed by the semi-automatic “SmartBreast” software (Mindray, Resona R9, 3–14 MHz transducer). The investigator was blinded to mammographic and previous ultrasound results. The analyses by “SmartBreast”, in particular, involved the following parameters provided by the BI-RADS lexicon for each lesion: dimensions (mm), shape (oval, rounded, irregular), orientation (parallel, not parallel), margins (circumscribed or not circumscribed: indistinct, angular, microlobulated, spiculated), echo-pattern (anechoic, isoechoic, hypoechoic, hy-

perechoic, heterogeneous, complex cystic, and solid mass), posterior features (no features, enhancement, shadowing, combined pattern), microcalcifications, and vascularization at color Doppler (absent, peripheral, internal). All these ultrasound features were automatically detected and analyzed by the software, which, at the end, provided a summary table with the determination of a BI-RADS category and the consequent probability of benignity or suspicion of malignancy (Figure 1).

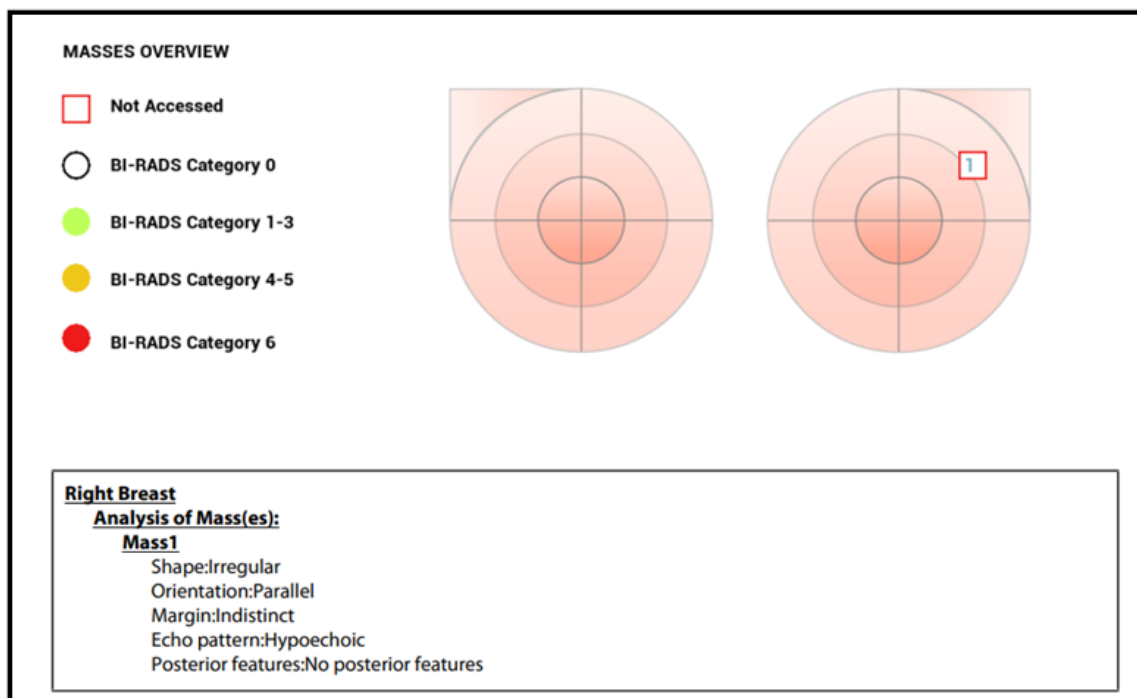


Figure 1. Mass overview with BI-RADS score provided by “SmartBreast”.

In the same ultrasound session, the investigator also performed elastography using the three main techniques: SE (qualitative and semi-quantitative method with SR), 2D SWE (Kpa and m/s), and pSWE (Kpa). At least five measurements were performed for every elastographic technique in each breast nodule.

Every elastographic evaluation included a quality bar that indicated the correct execution of the exam. The ROI was placed in the lesion, including as much tumoral area as possible. In both 2D SWE and pSWE analyses, the ROI was placed at least 3 mm below the skin surface; more superficial evaluations make the elastography examination unreliable.

SE was performed, taking care not to apply any pre-compression. The ultrasound probe was kept perpendicular to the skin surface using a real-time quality indicator to control the optimal sequence of compression–release. Elastography and B-mode images were visible simultaneously on the display (double view) in order to evaluate the qualitative parameters of the color scale. When the compression–release cycles had been completed and the optimal dynamics had been obtained through a real-time quality indicator, the maximum decompression point was selected in post-processing, and a region of interest (ROI) was manually positioned into the lesion, trying to include most of the lesion without the surrounding tissue. A second ROI, approximately equal in size to the first one, was placed on the normal fat tissue near the lesion at the same depth, avoiding possible motion artifacts. Then, the software inside the ultrasound machine calculated the strain ratio value, given by the deformability of the lesion in comparison to the fat tissue, thus providing semi-quantitative information (Figure 2b).

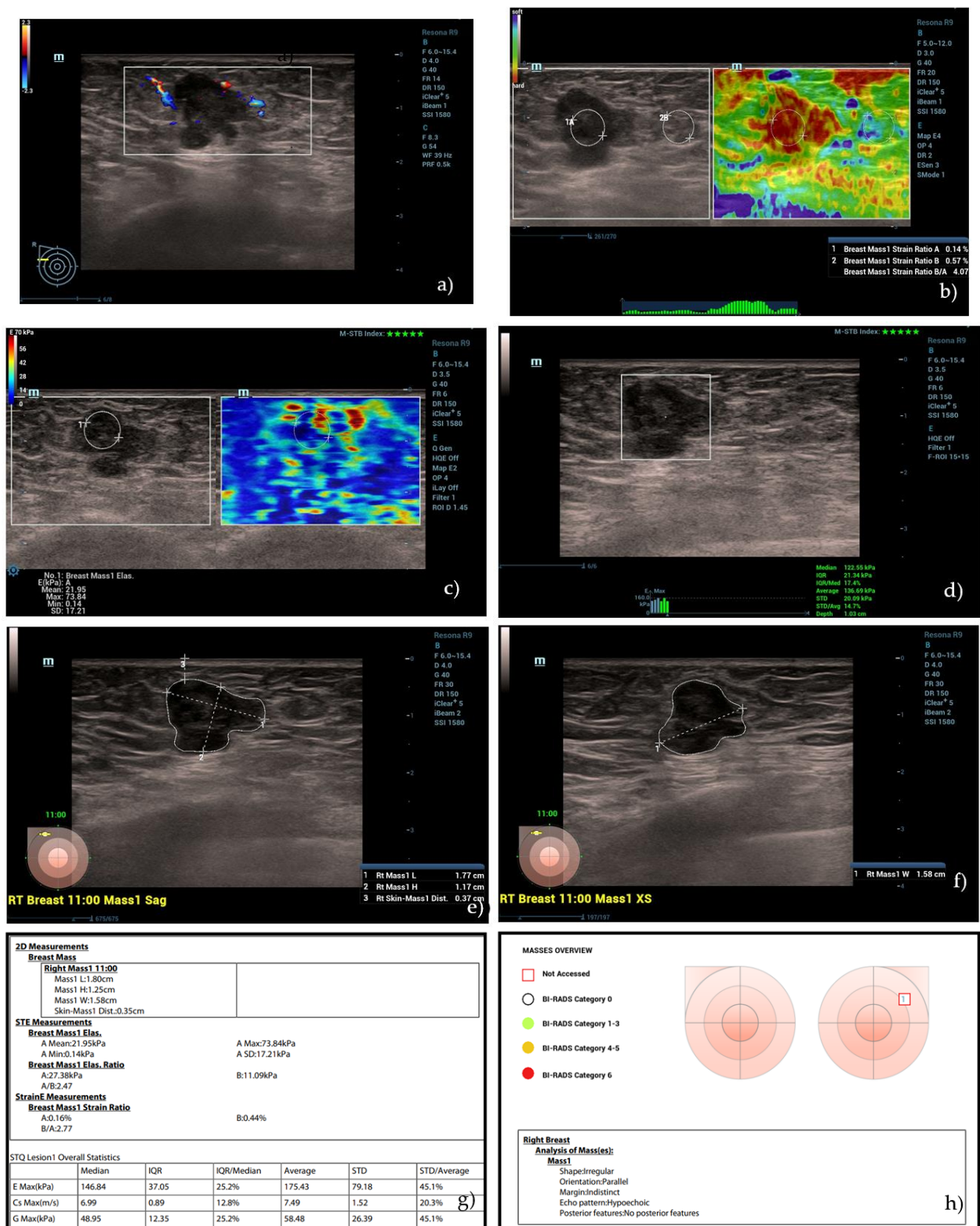


Figure 2. (a) A hypoechoic lesion with irregular margins and vascular internal signs at color Doppler evaluation, classified as BI-RADS 5 by human operator. (b) Semi-quantitative elastography showing a value of strain ratio (4.07) suggestive of stiff lesion. (c) The same lesion, showing intermediate values at 2D SWE evaluation (21.95 kPa) and (d) high values at pSWE analysis (122.55 kPa). (e–h) “SmartBreast” assessment, suggestive of malignancy. At histological evaluation, it was a B5 lesion (infiltrating ductal carcinoma).

Subsequently, the lesion was evaluated using the 2D SWE technique. The investigator positioned the transducer so that it remained stable and perpendicular to the lesion without any pressure while maintaining only slight contact with the skin in order to minimize compression artifacts. The patient was instructed to maintain a short inspiratory apnea to avoid respiratory motion artifacts. A mechanical impulse from the probe generated shear waves in the breast tissue, and their propagation was analyzed in a real-time color map. In this technique, the impulse coming from the transducer generates a downward displacement of the tissue parallel to each grid, and the speed of propagation of the shear waves can be measured (m/s). Breast lesion stiffness was assessed by placing an ROI in the lesion and was expressed in kPa. The ROI was placed in the lesion so as to include as much tumoral area as possible, avoiding the loss of signal due to artifacts (Figure 2).

The pSWE assessment was based on the same physical principle of 2D SWE single-point stiffness was measured at different points of the lesion instead of an area. Each patient was asked to hold their breath, and the operator positioned the transducer perpendicular to the lesion without any pressure, waiting for the machine to take from 5 to 10 measurements at different points of the breast nodule in order to obtain a representation of the stiffness, expressed in Kpa, through maximum, minimum, and median values. The pSWE evaluation also included a quality bar that indicated the correct execution of the same (Figure 2d).

The histopathological examination was considered the gold standard of reference; therefore, all breast lesions underwent core-needle biopsy and/or surgery.

Ultrasound-guided biopsy was performed under local anesthesia with a 14-gauge needle (Precisa, HS), and at least three tissue samples were collected for each breast lesion [15]. Every biopsy sample was placed in formalin and analyzed by a pathologist specializing in the diagnosis of breast cancer (with at least 15 years of experience). The pathologist was blinded to the ultrasound results.

Statistical Analysis

The Bland–Altman method was used for the analysis of continuous data and for the evaluation of software–investigator agreement. Lin’s concordance coefficient and Cohen’s k were also calculated for each breast lesion parameter predicted by the BI-RADS lexicon.

To determine the diagnostic accuracy of conventional B-mode ultrasound, BI-RADS category, SE, 2D SWE, and pSWE in breast disease, 2×2 contingency tables were used, and the area under the curve (AUC) ROC was calculated. Optimal cut-off values were calculated to optimize the sensitivity and specificity of strain elastography (SE) with strain ratio (SR) and shear wave elastography (2D SWE and pSWE) using the Youden index.

All statistical calculations were carried out using Stata software (12.0 version, Stata Corporation, College Station, TX, USA).

3. Results

The histological examination identified 22 benign breast lesions (23/92, 25%), 7 lesions classified as B3 (7/92, 7.6%), and 62 malignancies (62/92, 67.3%). Benign lesions included fibroadenomas (13), fibrocystic mastopathy (6), adenosis (2), fibrotic lesions (1), and inflammatory lesions (1). B3 nodules included atypical (1) and typical (1) intraductal papilloma, sclerosing adenosis (3), and atypical ductal hyperplasia (2). The malignant tumors included infiltrating ductal carcinomas (30), infiltrating ductal carcinomas with foci of in situ ductal carcinoma (18), ductal carcinoma in situ (3), invasive lobular carcinomas (7), infiltrating mucinous carcinoma of mixed type with foci of ductal carcinoma in situ (3), and pleomorphic sarcoma (1).

In the analysis of BI-RADS parameters, Lin’s correlation coefficient showed a moderate agreement between the “SmartBreast” and the operator in the evaluation of the dimensions (0.90, $p = 0.07$), as also seen in the Bland–Altman agreement in Figure 3.

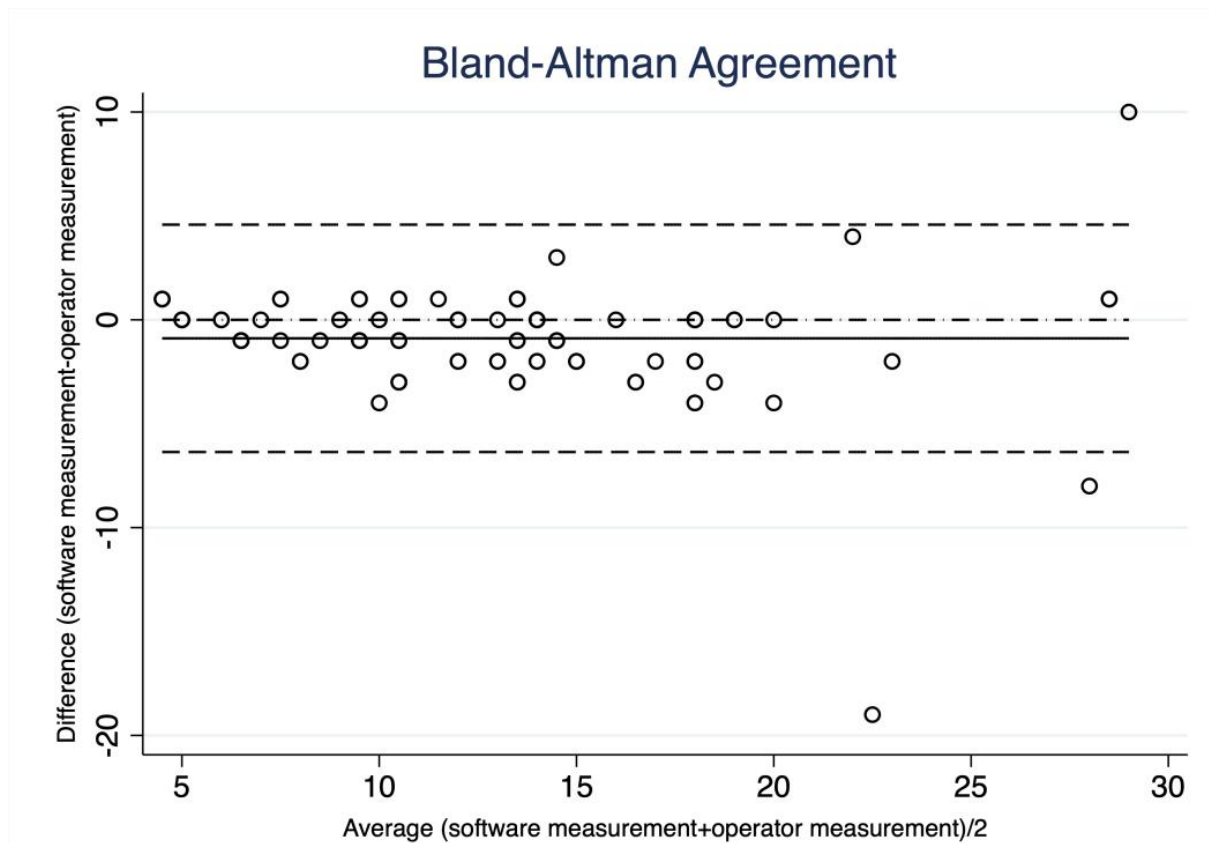


Figure 3. Bland–Altman correlation. Breast lesion diameters measured by “SmartBreast” and by radiologist. The B-A plot represents every difference between the measurement by the software and the measurement by the operator (Y-axis) against the average of the measurement (X-axis). Most of the points, except three, lie between the two confidence limits (lower limit: mean difference-2 SD; upper limit: mean difference + 2SD), on both the lower and higher average values (good agreement).

Calculating Cohen’s *k* for the other BI-RADS parameters, the following criteria were used: if *k* assumed values between 0 and 0.4, the agreement was considered poor; if *k* assumed values between 0.4 and 0.6, the agreement was moderate; if *k* values were between 0.6 and 0.8, the agreement was good; if *k* values were between 0.8 and 1, the agreement was considered excellent.

In our study, the agreement between the software and the investigator was excellent in the identification of the posterior features of breast lesions (Cohen’s *k* = 0.94); good in the evaluation of the shape and vascular signal at color Doppler (Cohen’s *k*, respectively, of 0.6 and 0.65); and poor in the analysis of orientation, margins, and echo-pattern (Cohen’s *k*, respectively, of 0.28, 0.33, and 0.48). In the identification of microcalcifications, Cohen’s *k* was 0.36, with the area under the ROC curve equal to 0.64.

The analysis of the agreement in the definition of the final BI-RADS score between the software and the human investigator showed a Cohen’s *k* of 0.35 (poor), 0.28 between the software and the histological results (poor), and 0.71 between the operator and the histological results (good).

Elastography analysis in the discrimination between malignant and benign lesions showed an AUC of 0.84 for the strain ratio, 0.64 for the 2D SWE, and 0.61 for the pSWE, with the cut-off values respectively equal to 1.69 (sensitivity: 0.81, specificity: 0.86), 25 Kpa (sensitivity: 0.73, specificity: 0.55), and 64.34 kPa (sensitivity: 0.71, specificity: 0.50). The results are shown in Table 1.

Table 1. Comparison of methods and their combination. PPV—positive predictive value, NPV—negative predictive value, ROC area—receiver operating characteristic area.

Operator	Sensitivity (%)	Specificity (%)	ROC Area	PPV	NPV
Experienced radiologist	93.2%	75%	0.84	87.2%	85.7%
“SmartBreast”	78.8%	70.8%	0.81	85.4%	81%
Strain Ratio (SR) (cut-off = 1.69)	81%	86%	0.84	84.2%	80%
2D SWE (cut-off = 25 kPa)	73%	55%	0.64	78.9%	57.4%
pSWE (cut-off = 64.34 kPa)	71%	50%	0.61	71.1%	58.6%
SR + Experienced radiologist	94.5%	78.8%	0.80	85.5%	96.4%
SR + “SmartBreast”	79.3%	76.6%	0.82	84.7%	81.2%
SR + Experienced Radiologist + “SmartBreast”	98.8%	61.7%	0.83	82%	96.7%
2DSWE + Experienced radiologist	93.4%	75.5%	0.67	79.5%	85.8%
pSWE + “SmartBreast”	78%	62.3%	0.71	79.7%	66.4%
2D SWE + Experienced Radiologist + “SmartBreast”	88.6%	64.5%	0.66	78.3%	79.7%
pSWE + Experienced Radiologist	92.9%	68.9%	0.65	78.4%	68.3%
2D SWE + “SmartBreast”	75.6%	68.7%	0.55	77.8%	67.6%
pSWE+ Experienced Radiologist + “SmartBreast”	93.1%	71.8%	0.73	78.8%	69.4%

4. Discussion

The differential diagnosis of breast tumors is still a significant challenge despite new technological developments that have provided more helpful tools for the radiological distinction of cancer from benign lumps.

The BI-RADS lexicon, updated in the last version of 2013 by the American College of Radiology (ACR), aims to standardize the interpretation and reporting of breast imaging, including ultrasound examination [7]. Despite the validation of this system, the variability in the analysis of focal breast lesions is still a problem, in particular, for some of its descriptors, such as margins and echo-patterns of the lesions. For this reason, automatic and semi-automatic software and computer-aided artificial intelligence have been created in recent years in order to process the images and extract features that can be classified according to the algorithms used in each analysis phase.

According to some authors, these systems can potentially improve the classification of breast masses by increasing the radiologist’s performance. In a study by Buchbinder et al., a computer-aided system correctly upgraded malignant lesions initially assigned a BI-RADS 3 score at mammography to a BI-RADS 4 or 5 category at 90% [16]. However, a 2019 review by Le et al. that evaluated the potential role of artificial intelligence for supporting breast imaging in mammography, ultrasound, and MRI, showed a variability of the results found in the literature, focusing on the need to carry out large-scale cohort studies in order to have more data and to standardize the interaction with the automatic tools [14]. Shen et al. demonstrated that a computer-aided classification had a statistical improvement in the accuracy and specificity of US examination (5.91% and 8.85%, respectively) compared

to a radiologist alone [17]. In 2017, Kim et al. reported a higher and statistically significant AUC (0.725) of a series of 192 breast lesions assessed using a computer-aided system called S-Detect in comparison with an expert radiologist (0.653) ($p = 0.038$) [18]. Bartolotta et al. showed, in their study, that this software can lead to an increase in the number of breast masses correctly characterized by US, although this increase was not statistically significant [19]. A 2021 meta-analysis by Wang et al. indicated how the evaluation with the same type of CAD (S-Detect) could play a role in the distinction between benign and malignant lesions with high values of sensitivity and specificity (0.82 and 0.83, respectively) [20]. Liu et al. evaluated the role of S-Detect together with SWE, demonstrating that the differences in sensitivity, specificity, accuracy, and AUC of the three diagnostic methods were not statistically significant (all $p > 0, 05$), however, encouraging this technology as a tool in supporting young and less experienced radiologists in breast imaging evaluation [21]. Similar results were also reported in the previous work by Di Segni et al. [22]. A 2022 study by Lyu et al. showed that automatic ultrasound detection of BI-RADS 4 lesions performed by artificial intelligence had higher accuracy in determining benign and malignant tumors (0.87, 0.75, and 0.80, respectively, for sensitivity, specificity, and accuracy) than conventional ultrasound (0.85, 0.67, and 0.75, respectively) [23].

It is noteworthy that, to date, there are no papers in the literature that evaluate the role of the new “SmartBreast” in the discrimination of the individual BI-RADS lexicon descriptors or the combined role of the software together with the different elastography techniques in the assessment of the final BI-RADS score.

The results of our study showed a moderate agreement between the “SmartBreast” software and the human investigator in the evaluation of tumor dimensions (Lin’s coefficient = 0.90, $p = 0.07$).

A good agreement was found in the identification of the posterior features and in the evaluation of the shape and the analysis of vascular signals at color Doppler (Cohen’s k of 0.94, 0.6, and 0.65, respectively). The agreement was found to be lower in the analysis of the most difficult BI-RADS parameters, such as orientation, margins, and echo pattern of the breast masses (Cohen’s k of 0.28, 0.33, and 0.48, respectively).

With regard to the identification of microcalcifications, the area under the ROC curve was equal to 0.64, despite a Cohen’s k value of 0.36, demonstrating a good agreement between the “SmartBreast” the human operator, and mammography.

The agreement in the definition of the BI-RADS final score was poor between software and operator (0.35) and between software and histological results (0.28), but it was good between operator and histological final assessment (0.71).

These data confirm the potential role of CAD systems in supporting breast lesion characterization for less experienced operators, but this system is neither of better diagnostic performance nor can it currently replace a radiologist with experience in breast cancer imaging. One of the limits found in our study that can partly explain these results is the presence of nine small lesions (9/92, 9.7%) ≤ 6 mm in size, for some of which the “SmartBreast” software was not able to correctly identify the lesion alone, or it did not correctly define the margins in consideration of the exceedingly small size.

Some studies have also evaluated the diagnostic role of elastography in breast nodule discrimination. In particular, some authors suggested that strain elastography may be complementary to the BI-RADS classification, increasing the performance of ultrasound [24,25]. Farrokh et al. [26] reported sensitivity values of 0.94 and specificity of 0.87 with a cut-off of 2.9 for SR. On the other hand, Alhabshi et al. [27] reported a cut-off value of 5.6 associated with the best diagnostic performance of SR. Therefore, it is evident how much the SR cut-off values are variable, and this variability is related to different equipment used, to operators’ experience, and to the lesions’ depth and size.

A further method, shear wave elastography (SWE), has been applied in breast lesion ultrasound analysis. A 2022 study by Wang et al. showed that the use of combined qualitative 2D SWE and/or color Doppler with BI-RADS had higher AUC values ($p < 0.001$) than BI-RADS alone and that, compared with BI-RADS alone, the sensitivity

slightly decreased, while the specificity, PPV, NPV, and accuracy were significantly improved [28]. Chang et al. [29] demonstrated that the mean elasticity value with SWE was significantly higher in malignant lesions (153 kPa \pm 58) compared with that of benign ones (46 kPa \pm 43), establishing an optimal cut-off value of 80 kPa.

In summary, both SE and 2D SWE have shown considerable potential for increasing diagnostic accuracy in the characterization of breast lesions. However, there are still only a few studies that have compared these techniques. Seo et al. [30] reported that the AUC for the elasticity values of strain elastography was slightly higher than that of 2D SWE but without a statistically significant difference (strain ratio 0.929, $p > 0.05$). Combined SE and 2D SWE showed significantly higher diagnostic accuracy than the methods used alone ($p = 0.031$). Fujioka et al. [31] indicated that the combined use of SE and 2D SWE together increased the performance of B-mode ultrasound alone. In particular, 2D SWE was more useful than SE. No statistically significant differences were found between the qualitative and quantitative assessments.

Another paper by Altintas et al. demonstrated that SE, 2D SWE, and pSWE had higher diagnostic performance individually than B-mode US alone for distinguishing between malignant and benign breast masses with similar diagnostic performance; the AUC for each of these elastography methods was 0.93, 0.93, 0.98, 0.97, 0.98, and 0.96, respectively ($p < 0.001$ for all measurements) [32].

In our study, strain elastography (cut-off = 1.69) showed a greater AUC than 2D SWE and pSWE (equal to 0.84, 0.64, and 0.61, respectively), with a sensitivity comparable to pSWE (respectively, of 0.81 and 0.84) but with a greater specificity (respectively, of 0.86 and 0.55), proving to be an accurate method in the discrimination between benign and malignant breast lesions. The association between SR, an experienced radiologist, and “SmartBreast” had the best sensitivity amongst the different methods (0.99), despite less specificity (0.62) that was the best for SR taken alone (0.86), demonstrating that SR is a valid ultrasound method. pSWE showed the lowest sensitivity and specificity (0.71 and 0.50, respectively), proving to be the worst elastographic method for breast lesion evaluation in our study.

These data could be related to the high prevalence of malignancies in our cohort and to the technology we used, for which there are still no universal cut-offs for stiffness values to be used, but they confirmed the potential role of these technologies in supporting the radiologist’s diagnosis in the evaluation of breast focal lesions.

5. Conclusions

Our study showed that multiparametric ultrasound evaluation of focal breast lesions is feasible and may increase their characterization. In particular, the semi-quantitative evaluation with SR significantly improves the diagnostic performance of the BI-RADS classification, having the association SR + experienced radiologist + “SmartBreast” with, in our study, a sensitivity of 0.99, while SR alone had a sensitivity of 0.81 and a specificity of 0.86. The semi-automatic “SmartBreast” Resona R9, Mindray software showed a good agreement with the investigator in our preliminary results, considering size (Lin’s correlation coefficient of 0.90, $p = 0.07$), shape, vascularization, and posterior features during nodule evaluation (Cohen’s k of 0.6, 0.65, and 0.94, respectively), except for the margins, echo pattern, and orientation (Cohen’s k of 0.33, 0.48, and 0.28, respectively). The automatic analysis, therefore, did not statistically increase the diagnostic performance, either alone or in association with elastographic methods, but it could have a role in guiding and training young, less experienced radiologists.

Further studies are needed to validate the results of our work, taking into consideration a greater number of breast lesions in multicenter studies.

Author Contributions: Conceptualization, O.G., V.C., L.B., F.P. and V.R.; methodology, V.C., O.G., A.R. and F.P.; software, V.C. and O.G.; validation, V.C., O.G. and C.D.V.; formal analysis, C.D.V. and O.G.; investigation, O.G. and V.C.; resources, M.V., F.P., L.B., L.C., F.T., V.R. and A.S.; data curation, O.G.; writing—original draft preparation, O.G., A.R. and D.F.; writing—review and editing V.C., M.V., G.V., C.C., M.D.S. and V.R.; visualization, O.G.; supervision, V.C.; project administration, V.C. and M.V. All authors have read and agreed to the published version of the manuscript.

Funding: This research received no external funding.

Institutional Review Board Statement: The study was conducted in accordance with the Declaration of Helsinki.

Informed Consent Statement: Informed consent was obtained from all subjects involved in the study.

Data Availability Statement: The data presented in this study are available on request from the corresponding author.

Conflicts of Interest: The authors declare no conflict of interest.

References

- Ghoncheh, M.; Pournamdar, Z.; Salehiniya, H. Incidence and Mortality and Epidemiology of Breast Cancer in the World. *Asian Pac. J. Cancer Prev.* **2016**, *17*, 43–46. [[CrossRef](#)]
- Kashyap, D.; Pal, D.; Sharma, R.; Garg, V.K.; Goel, N.; Koundal, D.; Zaguia, A.; Koundal, S.; Belay, A. Global Increase in Breast Cancer Incidence: Risk Factors and Preventive Measures. *BioMed Res. Int.* **2022**, *2022*, 9605439. [[CrossRef](#)] [[PubMed](#)]
- Lauby-Secretan, B.; Scoccianti, C.; Loomis, D.; Benbrahim-Tallaa, L.; Bouvard, V.; Bianchini, F.; Straif, K. Breast-Cancer Screening—Viewpoint of the IARC Working Group. *N. Engl. J. Med.* **2015**, *372*, 2353–2358. [[CrossRef](#)] [[PubMed](#)]
- Humphrey, L.L.; Helfand, M.; Chan, B.K.; Woolf, S.H. Breast Cancer Screening: A Summary of the Evidence for the U.S. Preventive Services Task Force. *Ann. Intern. Med.* **2002**, *137*, 347–360. [[CrossRef](#)]
- Smith, R.A. An Overview of Mammography: Benefits and Limitations. *J. Natl. Compr. Cancer Netw.* **2003**, *1*, 264–271. [[CrossRef](#)]
- Moss, H.A.; Britton, P.D.; Flower, C.D.; Freeman, A.H.; Lomas, D.J.; Warren, R.M. How reliable is modern breast imaging in differentiating benign from malignant breast lesions in the symptomatic population? *Clin. Radiol.* **1999**, *54*, 676–682. [[CrossRef](#)]
- D’Orsi, C.J.; Sickles, E.A.; Mendelson, E.B.; Morris, E.A. *ACR BI-RADS® Atlas, Breast Imaging Reporting and Data System*; American College of Radiology: Reston, VA, USA, 2013.
- Barr, R.G.; Destounis, S.; Lackey, L.B.; Svensson, W.E.; Balleyguier, C.; Smith, C. Evaluation of breast lesions using sonographic elasticity imaging: A multicenter trial. *J. Ultrasound Med.* **2012**, *31*, 281–287. [[CrossRef](#)]
- Cosgrove, D.; Piscaglia, F.; Bamber, J.; Bojunga, J.; Correas, J.M.; Gilja, O.A.; Klauser, A.S.; Sporea, I.; Calliada, F.; Cantisani, V.; et al. EFSUMB guidelines and recommendations on the clinical use of ultrasound elastography. Part 2: Clinical applications. *Ultraschall. Med.* **2013**, *34*, 238–253.
- Cosgrove, D.; Barr, R.; Bojunga, J.; Cantisani, V.; Chammas, M.C.; Dighe, M.; Vinayak, S.; Xu, J.-M.; Dietrich, C.F. WFUMB Guidelines and Recommendations on the Clinical Use of Ultrasound Elastography: Part 4. Thyroid. *Ultrasound Med. Biol.* **2017**, *43*, 4–26. [[CrossRef](#)]
- Grajo, J.R.; Barr, R.G. Strain elastography for prediction of breast cancer tumor grades. *J. Ultrasound Med.* **2014**, *33*, 129–134. [[CrossRef](#)]
- Barr, R.G.; Zhang, Z. Shear-Wave Elastography of the Breast: Value of a Quality Measure and Comparison with Strain Elastography. *Radiology* **2015**, *275*, 45–53. [[CrossRef](#)] [[PubMed](#)]
- Săftoiu, A.; Gilja, O.H.; Sidhu, P.S.; Dietrich, C.F.; Cantisani, V.; Amy, D.; Bachmann-Nielsen, M.; Bob, F.; Bojunga, J.; Brock, M.; et al. The EFSUMB Guidelines and Recommendations for the Clinical Practice of Elastography in Non-Hepatic Applications: Update 2018. *Ultraschall. Med.* **2019**, *40*, 425–453. [[CrossRef](#)] [[PubMed](#)]
- Le, E.; Wang, Y.; Huang, Y.; Hickman, S.; Gilbert, F. Artificial intelligence in breast imaging. *Clin. Radiol.* **2019**, *74*, 357–366. [[CrossRef](#)]
- Harvey, J.A.; Moran, R.E. US-guided core needle biopsy of the breast: Technique and pitfalls. *RadioGraphics* **1998**, *18*, 867–877. [[CrossRef](#)]
- Buchbinder, S.S.; Leichter, I.S.; Lederman, R.B.; Novak, B.; Bamberger, P.N.; Sklair-Levy, M.; Yarmish, G.; Fields, S.I. Computer-aided classification of BI-RADS category 3 breast lesions. *Radiology* **2004**, *230*, 820–823. [[CrossRef](#)] [[PubMed](#)]
- Shen, W.C.; Chang, R.F.; Moon, W.K. Computer aided classification system for breast ultrasound based on breast imaging reporting and data system (BI-RADS). *Ultrasound Med. Biol.* **2007**, *33*, 1688–1698. [[CrossRef](#)]
- Kim, K.; Song, M.K.; Kim, E.K.; Yoon, J.H. Clinical application of S-Detect to breast masses on ultrasonography: A study evaluating the diagnostic performance and agreement with a dedicated breast radiologist. *Ultrasonography* **2017**, *36*, 3–9. [[CrossRef](#)]

19. Bartolotta, T.V.; Orlando, A.; Cantisani, V.; Matranga, D.; Ienzi, R.; Cirino, A.; Amato, F.; Di Vittorio, M.L.; Midiri, M.; Lagalla, R. Focal breast lesion characterization according to the BI-RADS US lexicon: Role of a computer-aided decision-making support. *Radiol. Med.* **2018**, *123*, 498–506. [[CrossRef](#)]
20. Wang, X.; Meng, S. Diagnostic accuracy of S-Detect to breast cancer on ultrasonography: A meta-analysis (PRISMA). *Medicine* **2022**, *101*, e30359. [[CrossRef](#)]
21. Liu, M.; He, F.; Xiao, J. Application of S-detect combined with virtual touch imaging quantification in ultrasound for diagnosis of breast mass. *Zhong Nan Da Xue Xue Bao Yi Xue Ban* **2022**, *47*, 1089–1098.
22. Di Segni, M.; de Soccio, V.; Cantisani, V.; Bonito, G.; Rubini, A.; Di Segni, G.; Lamorte, S.; Magri, V.; De Vito, C.; Migliara, G.; et al. Automated classification of focal breast lesions according to S-detect: Validation and role as a clinical and teaching tool. *J. Ultrasound* **2018**, *21*, 105–118. [[CrossRef](#)]
23. Lyu, S.-Y.; Zhang, Y.; Zhang, M.-W.; Zhang, B.-S.; Gao, L.-B.; Bai, L.-T.; Wang, J. Diagnostic value of artificial intelligence automatic detection systems for breast BI-RADS 4 nodules. *World J. Clin. Cases* **2022**, *10*, 518–527. [[CrossRef](#)]
24. Chiorean, A.; Duma, M.M.; Ducea, S.M.; Iancu, A.; Dumitriu, D.; Roman, R.; Sfrangeu, S. Real-time ultrasound elastography of the breast: State of the art. *Med. Ultrason.* **2008**, *10*, 73–82.
25. Tan, S.M.; Teh, H.S.; Mancner, J.K.; Poh, W.T. Improving B mode ultrasound evaluation of breast lesions with real-time ultrasound elastography—A clinical approach. *Breast* **2008**, *17*, 252–257. [[CrossRef](#)] [[PubMed](#)]
26. Farrokh, A.; Wojcinski, S.; Degenhardt, F. Diagnostic value of strain ratio measurement in the differentiation of malignant and benign breast lesions. *Ultraschall. Med.* **2011**, *32*, 400–405. [[CrossRef](#)]
27. Alhabshi, S.M.I.; Rahmat, K.; Halim, N.A.; Aziz, S.; Radhika, S.; Gan, G.C.; Vijayanathan, A.; Westerhout, C.J.; Mohd-Shah, M.N.; Jaszle, S.; et al. Semi-Quantitative and Qualitative Assessment of Breast Ultrasound Elastography in Differentiating Between Malignant and Benign Lesions. *Ultrasound Med. Biol.* **2013**, *39*, 568–578. [[CrossRef](#)]
28. Wang, B.; Chen, Y.-Y.; Yang, S.; Chen, Z.-W.; Luo, J.; Cui, X.-W.; Dietrich, C.F.; Yi, A.-J. Combined Use of Shear Wave Elastography, Microvascular Doppler Ultrasound Technique, and BI-RADS for the Differentiation of Benign and Malignant Breast Masses. *Front. Oncol.* **2022**, *12*, 906501. [[CrossRef](#)]
29. Chang, J.M.; Moon, W.K.; Cho, N.; Yi, A.; Koo, H.R.; Han, W.; Noh, D.Y.; Moon, H.G.; Kim, S.J. Clinical application of shear wave elastography (SWE) in the diagnosis of benign and malignant breast diseases. *Breast Cancer Res. Treat.* **2011**, *129*, 89–99. [[CrossRef](#)]
30. Seo, M.; Ahn, H.S.; Park, S.H.; Lee, J.B.; Choi, B.I.; Sohn, Y.-M.; Shin, S.Y. Comparison and Combination of Strain and Shear Wave Elastography of Breast Masses for Differentiation of Benign and Malignant Lesions by Quantitative Assessment: Preliminary Study. *J. Ultrasound Med.* **2018**, *37*, 99–109. [[CrossRef](#)]
31. Fujioka, T.; Mori, M.; Kubota, K.; Kikuchi, Y.; Katsuta, L.; Kasahara, M.; Oda, G.; Ishiba, T.; Nakagawa, T.; Tateishi, U. Simultaneous comparison between strain and shear wave elastography of breast masses for the differentiation of benign and malignant lesions by qualitative and quantitative assessments. *Breast Cancer* **2019**, *26*, 792–798. [[CrossRef](#)]
32. Altıntaş, Y.; Bayrak, M.; Alabaz, Ö.; Celiktaş, M. A qualitative and quantitative assessment of simultaneous strain, shear wave, and point shear wave elastography to distinguish malignant and benign breast lesions. *Acta Radiol.* **2021**, *62*, 1155–1162. [[CrossRef](#)] [[PubMed](#)]

Disclaimer/Publisher’s Note: The statements, opinions and data contained in all publications are solely those of the individual author(s) and contributor(s) and not of MDPI and/or the editor(s). MDPI and/or the editor(s) disclaim responsibility for any injury to people or property resulting from any ideas, methods, instructions or products referred to in the content.